이학석사 학위논문

흉선 T 세포 발달과 증식에서 CD36 의 역할 연구

The Roles of CD36 in Thymic T Cell Development and Proliferation

울산대학교대학원

의 과 학 과

이 여 경

흉선 T 세포 발달과 증식에서 CD36 의 역할 연구

지도교수 정동환

이 논문을 이학석사학위 논문으로 제출함

2024 년 02 월

울산대학교 대학원

의 과 학 과

이 여 경

이 여 경의 이학석사학위 논문을 인준함

심사위원 황 신 (인)

심사위원 정 동 환 (인)

심사위원 김 나 영 (인)

울 산 대 학 교 대 학 원

2024 년 02 월

Contents

그림목차

Abstract

Background: CD36, also known as fatty acid translocase and scavenger receptor, is a transmembrane molecule which functions as signaling molecule and lipid transporter. CD36 binds oxidized low-density lipoprotein (ox-LDL), long chain fatty acid, damage-associated molecular pattern (DAMP), and pathogen-associated molecular pattern (PAMP). CD36 is expressed not only in fat cells, muscle cells, and endothelial cells, but also in immune cells such as platelets, red blood cells, macrophages, dendritic cells, and T cells. CD36 expressed in immune cells is known to play a role in immune metabolism, but its function in T cell development has been less elucidated.

Methods: CD36-floxed mice and Lck-cre mice were crossed to generate T-cell-specific CD36 knock-out (KO) mice, which were named CD36 conditional KO (cKO) mice. The thymus, spleen, and bone marrow cells of 3-4 week-old CD36 cKO mice and thymocytes of 5-8 week-old CD36 cKO mice were analyzed by flow cytometry. T cell proliferation was assessed by

carboxyfluorescein succinimidyl ester (CFSE) dilution and cell counting kit 8 (CCK8) assay in the presence of IL-2, anti-CD3, and anti-CD28 monoclonal antibodies. To investigate the mechanism underlying increased T cell proliferation, the activation of AKT, mTOR, and ERK was observed by flow cytometry. RNA was extracted from thymus and bone marrow cells and mRNA sequencing was performed.

Results: Three- to four-week-old CD36 cKO mice displayed increases in $CD3^+$, double negative (DN), DN3, $CD3^+$ double positive (DP) and CD8 single positive (SP) cells and reduction in DN4, total DP, $CD3^-$ DP and CD4 SP cells in the thymus. CD36 cKO splenocytes had lower frequency of CD4 SP cells, compared with WT. The frequency and mean fluorescence index (MFI) of $CD3^+$ bone marrow cells from CD36 cKO mice were lower than those of WT. Thymic T cells from CD36 cKO mice were more proliferative than those of WT upon CD3 and CD28 stimulation. mRNA-sequencing data showed that the expressions of *Ccl17* and *Ccr7* were upregulated, and those of *Ccl22* and *Ccr9* were downregulated in CD36 cKO thymus. It was confirmed by quantitative real-time PCR (qRT-PCR) that the expressions of *Ccl22* and *Ccr9*

were significantly decreased in CD36 cKO thymocytes, compared with those of WT. *Ccl17* and *Ccr7* expressions were higher and *Ccl22* and *Ccr9* expressions were lower in the CD36 cKO bone marrow than in WT, although the differences were not statistically significant.

Conclusion: CD36 cKO 3-4 week-old mice had defects in DN3 to DN4 transition. CD36 cKO thymic T cells were more proliferative than WT. The developmental changes of thymic T cells might result from the changes of the expression of chemokines and chemokine receptors. This study suggests that CD36 is a potential contributor to thymic T cell development from DN stage and has a regulatory function in proliferation.

Introduction

CD36 is a transmembrane glycoprotein that is also known as fatty acid translocase and scavenger receptor class B member 3 [1]. CD36 binds thrombospondin-1, damage-associated molecular patterns (DAMPs), pathogen-associated molecular patterns (PAMPs), oxidized low-density lipoproteins (ox-LDLs), and long-chain fatty acids [2]. It is expressed in various cell types including adipocytes, myocytes, endothelial cells, platelets, erythrocytes, macrophages, monocytes, dendritic cells, and T cells [3]. As CD36 is expressed in those cells and binds multiple ligands, it exerts multifunction associated with lipid metabolism and cell signaling, including immune-metabolic functions. CD36 plays a functional role in lipoprotein and fatty acid metabolism. The early research reveals that CD36 null mice significantly impair in the binding and uptake of ox-LDL as well as in the transport of long-chain fatty acids [4].

In immune system, macrophage CD36 mediates lipid uptake and the formation of foam cells in atherosclerosis and phagocytosis [5, 6]. On dendritic cells, CD36 recognizes,

phagocytoses apoptotic cells, and affects T cell priming [7]. CD36 mediates the uptake of fatty acids in tumor infiltrating $CD8^+$ T cells and it promotes lipid peroxidation and ferroptosis, which are associated with impaired $CD8^+$ T cell cytotoxic function and antitumor activity [8]. The expression of CD36 is upregulated in intratumoral Treg cells, that allows to uptake fatty acids within tumor microenvironment and promote mitochondrial fitness through peroxisome proliferator-activated receptor-β (PPAR-β)-dependent mechanism. Genetic ablation of CD36 in Treg cells impairs intratumoral Treg function, improving antitumor activity [9]. However, the role of CD36 in T cell development remains poorly understood.

T cells develop through a serial process in which bone marrow-derived hematopoietic progenitor cells enter the thymus, where they are matured and selected by migrating from the cortex to the medulla, and egress to the periphery and the tissues [10]. In the bone marrow, hematopoietic stem cells (HSCs), determined as $Lin^-Sca\text{-}1^+c\text{-}kit^+$, differentiate multipotent progenitors (MPPs) which have lost self-renewal capacity. MPPs generate common myeloid

progenitors (CMPs) and common lymphoid progenitors (CLPs) that have T lineage potential [11]. CLPs referred to as thymus seeding progenitors (TSPs) enter the thymus via the blood vessels at the junction of cortical and medullary regions [12]. After entering the thymus, TSPs become early T cell progenitors (ETPs) as double negative (DN) stage 1 thymocytes that lack the expressions of CD4 and CD8 and are defined as $CD44^{+}CD25^{-}$. Immature thymocytes go through $CD44^{+}CD25^{+}$ DN2 and $CD44^{-}CD25^{+}$ DN3 stages and migrate toward the subcapsular zone. DN3 thymocytes undergo T cell receptor (TCR)-β, TCR-γ, and TCR-δ chain gene rearrangements that promote to differentiate to the αβ lineage and γδ lineage [13]. Following the rearrangement of TCR-β chain, the TCR-β chain associates with the pre-TCR-α chain and CD3 signaling molecules to produce the pre-TCR complex [14]. This process called β-selection and the cell that fails this process undergoes apoptosis. It results in the expansion and transition of DN3 thymocytes to $CD44^{-}CD25^{-}$ DN4 and subsequently double-positive (DP) thymocytes expressing both CD4 and CD8. DN3 thymocytes which express TCR-γ and TCR-δ chain generate γδ-TCR and differentiate to γδ T cells [15]. DP thymocytes are located in the

cortex replace the pre-TCR-α chain with the TCR-α chain [16] and undergo positive selection that allows only T cells with TCRs that bind to MHC complexes expressed in thymic cells to survive. After positive selection, DP thymocytes mature to single positive (SP) cells through negative selection in the medulla. This leads to the apoptosis of immature cells with strong TCR signaling in response to self-MHC complexes [17]. Then, SP thymocytes, that recognize antigens and have self-tolerant immune function, exit from the thymus to the periphery [18].

T cell development, as well as T cell differentiation and activation, is dependent on energy metabolism. It is influenced by the uptake of nutrients. Lipid metabolism has been considered a regulator of T cell responses. The cells interact with environmental lipids and activate lipid intracellular signaling [19]. Lipid metabolism might be critical for maintaining thymic T cell development. For example, high-fat diet starting from young age impairs T cell development in the thymus and induces the apoptosis of thymocytes [20]. Glycerol-3-phosphate acyltransferase-1 gene ablation changes thymocyte lipid content, and it leads to the

reduction of thymic T cell production in mice [21]. Mice with deficiency of lysosomal acid lipases, which hydrolyze cholesterol esters and triglycerides to generate free fatty acids and cholesterols, have decreased thymocytes and defected T cell development in the thymus [22]. Those studies reveal lipid metabolisms in thymic microenvironments have a significant effect on the development of thymocytes. However, the function of CD36 in thymic T cell development has not been elucidated yet.

In this study, T-cell-specific CD36 knock-out (KO) mice, named CD36 conditional KO (cKO) mice, were utilized to determine whether CD36 is involved to thymic T-cell development. I investigated the phenotypes of thymocytes, bone marrow cells, and splenocytes from CD36 cKO mice and wild type (WT) mice, thymic T cell proliferation, and gene expressions of chemokines and chemokine receptors associated with T cell development, differentiation, and thymic egress. These results suggest that CD36 would be a potential contributor to T cell development, differentiation, and proliferation in the thymus.

Materials and Methods

Mouse

$Cd36^{tm1.1Ijg}$/J and B6.Cg-Tg(Lck-cre)548Jxm/J mice were purchased from Jackson Laboratory (Bar Harbor, ME, USA). All mice were on C57BL/6 background. Mice were crossed to generate T-cell-specific CD36 KO mice. CD36 cKO mice were bred under specific pathogen-free conditions. Experiments were performed at 3-8 weeks of age and studied in males and females. Wild type (WT) mice that were not ablated of exons 3 and 4 of CD36 gene were used as control. All experiments were approved by IACUC (Approval No.2022-14-288).

For genotyping, genomic DNA was extracted from the tail of mice. PCR was conducted by C1000 Touch Thermal Cycler (Bio-Rad, Hercules, CA, USA) using BioFACT 2X Lamp Taq PCR Master Mix 1 (BIOFACT, Daejeon, Republic of Korea). The primer sequences (from 5' to 3') are as follow: LoxP locus forward: ATTGGCATCTGTGTAGCGCTCTTGGC, LoxP locus reverse: TGCTACTATGCACTCCATGCAGGC, CD36 deletion forward: ATTGGCATCTGTGTAGCGCTCTTGGC, CD36 deletion reverse:

TCAGGACCATAGCAAGTAGGC [23], Cre forward: TGTGAACTTGGTGCTTGAGG, Cre reverse: CAGGTTCTTGCGAACCTCAT, Internal positive control (IPC) forward: CTAGGCCACAGAATTGAAAGATCT, IPC reverse: GTAGGTGGAAATTCTAG-CATCATCC. Since PCR assay for Lck-cre detection does not distinguish hemizygous, qRT-PCR was performed according to the Jackson Laboratory protocols. The primer sequences (from 5' to 3') are as follow: Cre forward: CAGTCAGGAGCTTGAATCCC, Cre reverse: CACTAAAGGGAACAAAAGCTGG, IPC forward: CACGTGGGCTCCAGCAT, IPC reverse: TCACCAGTCATTTCTGCCTTTG.

Isolation of thymocytes, splenocytes, and bone marrow cells

Thymus, spleen, and bone marrow were placed on cell strainers of pore size 100 μm (CORNING, Corning, NY, USA) and ground with the plunger of 1 ml syringe. Red blood cells (RBCs) were lysed with 1 x RBC lysis buffer (BioLegend, San Diego, CA, USA), Cells were suspended in RPMI 1640 (Welgene, Gyeongsan-si, Gyeongsangbuk-do, Republic of Korea)

supplemented with 10% inactivated FBS (Welgene), 100 U/mL penicillin, 100 μg/ml streptomycin (Welgene), 1 mM sodium pyruvate (Sigma Aldrich, St. Louis, MO, USA), and 55 μM 2-Mercaptoethanol (Gibco; Thermo Fisher Scientific, Waltham, MA, USA). The cell number was counted by trypan blue (Welgene) exclusion method using a hemocytometer.

Flow Cytometry

Isolated thymocytes, splenocytes, and bone marrow cells were blocked for non-specific Fc-mediated binding using purified rat anti-mouse CD16/CD32 (clone 2.4G2, BD Biosciences, San Diego, CA, USA), stained with antibodies, and washed twice with phosphate-buffered saline (PBS) (Biosesang, Seongnam-si, Gyeonggi-do, Republic of Korea) containing 2% FBS. Cells were stained with APC-conjugated anti-mouse CD45 (clone 30-F11, eBioscience; Thermo Fisher Scientific, Waltham, MA, USA) PerCP-Cy5.5 conjugated anti-CD3 (clone 145-2C11, eBioscience), BV510-conjugated anti-CD4 (clone FM4-5, BioLegend), BV650-conjugated anti-CD8 (clone 53-6.7, BioLegend), PE-conjugated anti-CD25 (clone PC61.5,

eBioscience), APC-conjugated anti-CD44 (clone IM7, BD Biosciences), PE-Cy7-conjugated anti-CD117 (clone ACK2, BioLegend), BV421-conjugated anti-CD34 (clone SA376A4, BioLegend), PE-Cy5-conjugated anti-TCR-β (clone H57-597, BioLegend), FITC-conjugated anti-CD3 (clone 145-2C11, BD Biosciences), PE-conjugated anti-CD8 (clone 53-6.7, eBioscience), PE-conjugated anti-phosphorylated-mTOR (clone MRRBY, eBioscience), BV421-conjugated anti-phosphorylated-AKT (clone M89-61, BD Biosciences), and Alexa Fluor 647-conjugated anti-phosphorylated-ERK (clone 6B8B69, BioLegend) monoclonal antibodies.

For intracellular staining, cells were fixed and permeabilized with BD Phosflow Lyse/Fix Buffer (5X) and BD Phosflow Perm Buffer III (BD Biosciences). After washing, Cells were detected by a CytoFLEX flow cytometer (Beckman Coulter Life Sciences, Brea, CA, USA) and analyzed using a FlowJo v10 software (Tree Star, Ashland, OR, USA).

T cell proliferation assay

T cell proliferation was assessed by CFSE dilution and CCK8 assay. Thymocytes were labeled with CFSE (Invitrogen, Thermo Fisher Scientific) and cultured at 1 x 10^6 cells/well in 24 well plates with 100 U/ml recombinant human IL-2 (rhIL-2; PeproTech, Rocky Hill, NH, USA), 1 μg/ml of mouse anti-CD3 (clone 145-2C11, BioLegend), and anti-CD28 (clone 37.51, Bio-Legend) monoclonal antibodies and rhIL-2 were treated every 2 days. On day 0, 3, and 5, CFSE dilution was detected by flow cytometry.

For CCK8 assay, cells were plated at 1 x 10^4 cells in triplicates in 96 well plates with rhIL-2, mouse anti-CD3, and anti-CD28 monoclonal antibodies. After 7 days, cells were treated with CCK8 reagent (Dojindo, Tabaru, Kumamoto, Japan) and the absorbance was measured using a microplate reader (TECAN, Männedorf, Switzerland) according to the man-ufacturer's instructions.

RNA isolation and qRT-PCR

RNA from thymocytes and bone marrow cells of CD36 cKO mice was extracted using TRIzol (Invitrogen). Complementary DNA (cDNA) was synthesized using Oligo(dT)12-18 Primer (Invitrogen), Superscript III reverse transcriptase (Invitrogen), 10 mM dNTP Mix (Invitrogen), and RNaseOUT Recombinant Ribonuclease Inhibitor (Invitrogen). qRT-PCR was performed by QuantStudio 5 Real-Time PCR system, 384-well (Applied Biosystems; Thermo Fisher Scientific) using cDNA mixtures with SYBR Green PCR Master Mix (Applied Biosystems). Results were normalized to the expression of *Gapdh* and *Hprt*. The primer sequences (from 5' to 3') are as follow: Gapdh forward: TTGTCAGCAATGCATCCTGCAC, Gapdh reverse: ACAGCTTTCCAGAGGGGCCATC [24], Hprt forward: TGCCGAGGATTTGGAAAAAGTG, Hprt reverse: AGAGGGCCACAATGTGATGG [25], Ccr7 forward: TCATTGCCGTGGTGGTAGTCTTCA, Ccr7 reverse: ATGTTGAGCTGCTTGCTGGTTTCG [26], Ccr9 forward: TGGCTTGTGTTCATTGTGGG, Ccr9 reverse: CAGAAGGGAAGAGTGGCAAG [27], Ccl17 forward: TTGTGTTCGCCTGTAGTGCATA, Ccl17 reverse: CAGGAAGTTGGTGAGCTGGTATA [28], Ccl22 forward:

AAGCCTGGCGTTGTTTTGAT, Ccl22 reverse: CCTGGGATCGGCACAGATA [29]. All primers were purchased by COSMOgenetech (Seoul, Republic of Korea).

RNA sequencing

RNA was extracted from thymocytes and bone marrow cells from CD36 cKO and WT mice as above. cDNA library was constructed using RiboCop rRNA Depletion and NEBNext Ultra II Directional RNA kit by Ebiogen (Seoul, Republic of Korea) for RNA sequencing. mRNA sequencing was performed using NovaSeq 6000 (Illumina, CA, USA). Venn diagram, clustering heatmap, and comparing gene expressions were generated using an exDEGA software (Ebiogen, Seoul, Republic of Korea).

Statistics

Statistical tests were performed by student *t*-test using a GraphPad Prism software (GraphPad Software, Inc., San Diego, CA, USA). CCK8 assay was analyzed by ordinary

two-way ANOVA followed by multiple comparisons. All data are shown as means ± SEM. *

$p < 0.05$, ** $p < 0.01$.

Results

CD36 cKO thymocytes of 3-4 week-old mice showed defects in T cell development.

To determine whether CD36 was involved in thymic T-cell development, I investigated the phenotypes of thymocytes from 3-4 week-old CD36 cKO mice and WT mice by flow cytometry. I used mice with Cre expression controlled by the *lck* promoter to generate T-cell-specific CD36 KO mice. The protein tyrosine kinase Lck is expressed in T cell lineages and critical for T cell development [30]. The gating strategy to analyze T cell phenotypes of the thymocytes is shown in Fig. 1A. The developmental stages are defined as DN, DP, CD4 SP and CD8 SP as previously described [31]. The percentages of $CD3^-$ thymocytes from CD36 cKO mice were decreased by approximately 0.96 fold, while those of $CD3^+$ thymocytes were increased by appreoximately 1.26 fold, compared with those of WT. The MFI of $CD3^+$ thymocytes were 1.72 fold higher in CD36 cKO mice than WT. The percentages of thymocytes from CD36 cKO mice were significantly increased by approximately 1.44 fold in the DN stage, but significantly decreased in the DP stage by approximately 0.95 fold, compared with WT.

CD36 cKO mice had 1.51-fold more percentages of DN3 thymocytes and 0.73-fold less percentages of DN4 stage than WT. CD36 cKO mice had 0.99-fold less percentages of $CD3^-$ DP cells and 1.27-fold more percentages of $CD3^+$ DP cells than WT. The percentages of CD4 SP cells were 0.82-fold less and CD8 SP cells were 1.25-fold more in CD36 cKO compared with WT. The differences in DN3, DN4, DP, and SP were statistically significant. The cell number of each stage from CD36 cKO was slightly increased than WT, but not statistically significant (Fig. 1B, Fig. 1C and D). The results suggest that CD36 cKO thymocytes have defects in DN3 to DN4 transition, possibly resulting in the accumulation of DN cells. CD36 cKO thymocytes of 3-4 week-old mice seemed to have problems in CD3 expression and progress to DP and SP.

To investigate whether developmental defects were specific in 3-4 week-old mice, flow cytometry was performed to analyze thymocytes in mice aged 5-8 weeks. No difference was found in frequencies, cell numbers, and $CD3^+$ MFI (Fig. 2A). These results indicate that development defects occur only in the thymus of 3-4 week-old mice, not in the adult mice.

The phenotypes of splenocytes from 3-4 week-old CD36 cKO mice and WT mice were observed by flow cytometry to identify any defects after thymic egress. The gating strategy of splenocytes is shown (Fig. 3A). The results display that CD4 SP cells from CD36 cKO mice were significantly decreased by approximately 0.72 fold, compared with WT. (Fig. 3B). In summary, the results suggest that development defects in the thymus might affect the phenotype of splenocytes in CD36 cKO mice.

Figure 1.

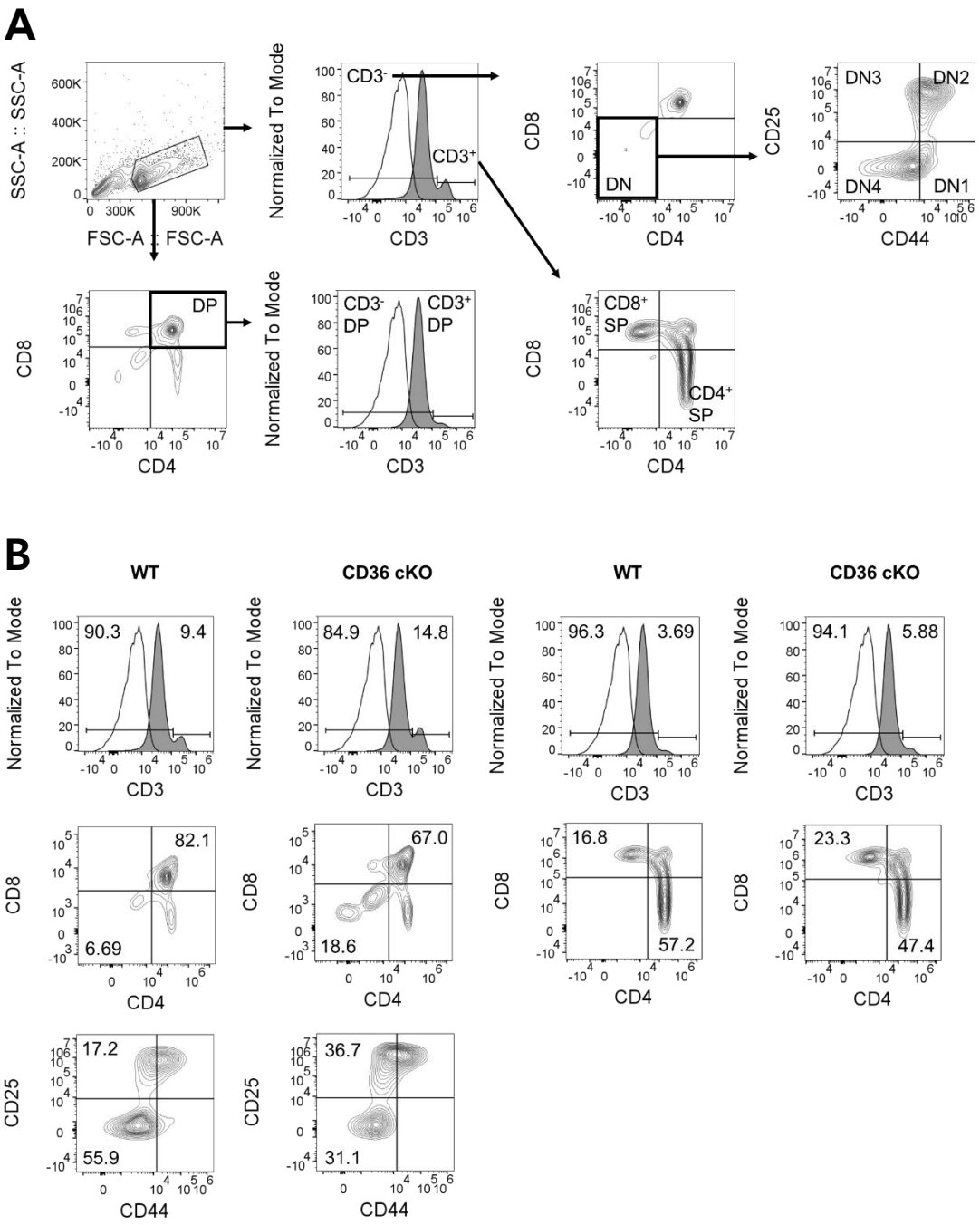
A
SSC-A :: SSC-A
FSC-A :: FSC-A
Normalized To Mode
CD3
CD3-
CD3+
CD8
CD4
DN
CD25
CD44
DN3
DN2
DN4
DN1
DP
CD3- DP
CD3+ DP
CD8+ SP
CD4+ SP
B
WT
CD36 cKO
90.3
9.4
84.9
14.8
96.3
3.69
94.1
5.88
82.1
6.69
67.0
18.6
16.8
57.2
23.3
47.4
17.2
55.9
36.7
31.1

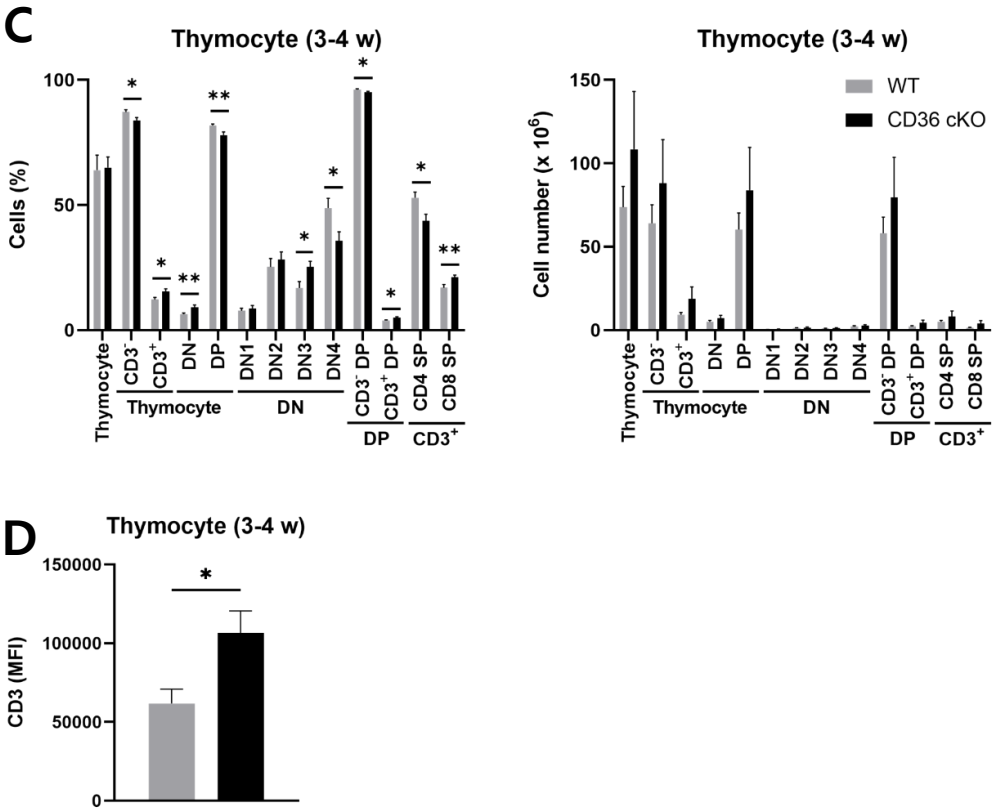

Figure 1. The phenotypes of thymic T cells in 3-4 week-old mice.

Flow cytometric analysis of thymocytes from 3-4 week-old CD36 cKO and WT mice. (A) Representative gating strategy was displayed. (B) Representative flow cytometric plots are shown. (C) The percentages and cell numbers of thymocyte subsets are shown (n = 9-14 per group). (D) The MFI of $CD3^+$ thymocytes are shown (n = 8-13 per group). Data are shown as mean ± SEM. * $p < 0.05$, ** $p < 0.01$. DN, double negative. DP, double positive. MFI, Mean fluorescence indice.

Figure 2.

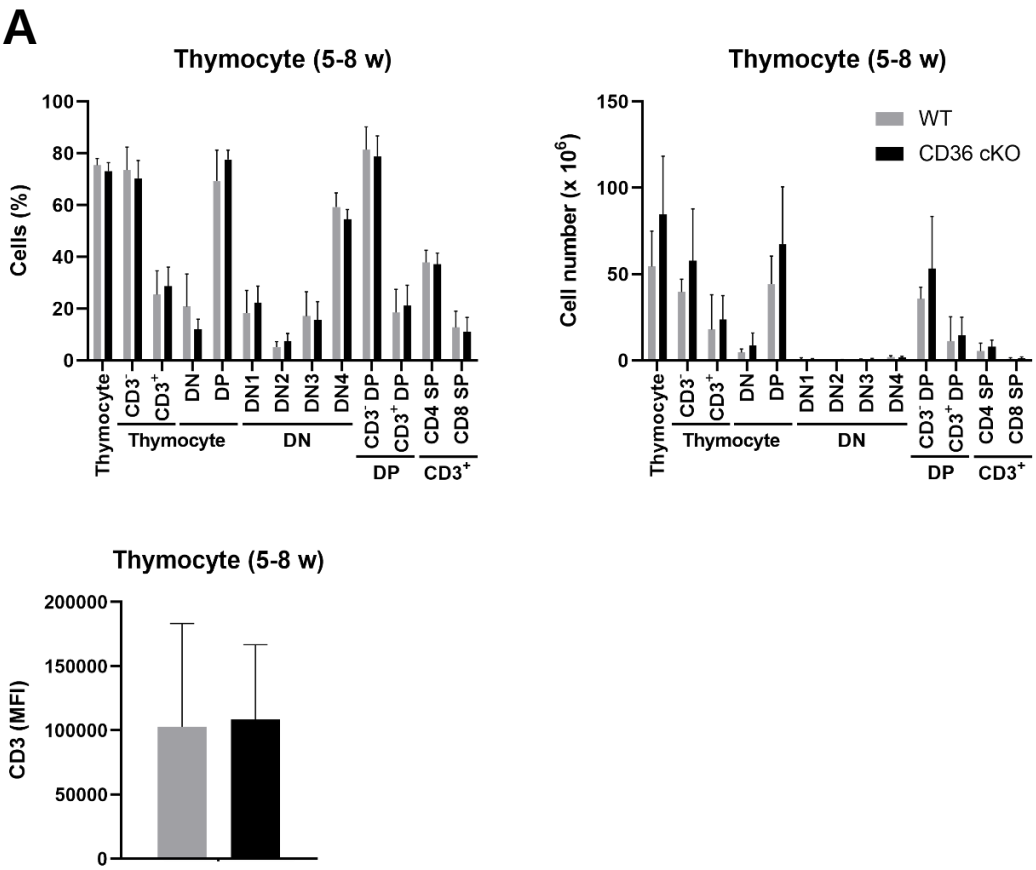

Figure 2. The phenotypes of thymic T cells in adults.

Flow cytometric analysis of thymocytes from 5-8 week-old CD36 cKO and WT mice. (A) The percentages, cell numbers of thymocytes' subset and the MFI of $CD3^+$ thymocytes from 5-8 week-old CD36 cKO and WT mice are shown (n = 4-7 per group). Data are shown as mean ± SEM.

Figure 3.

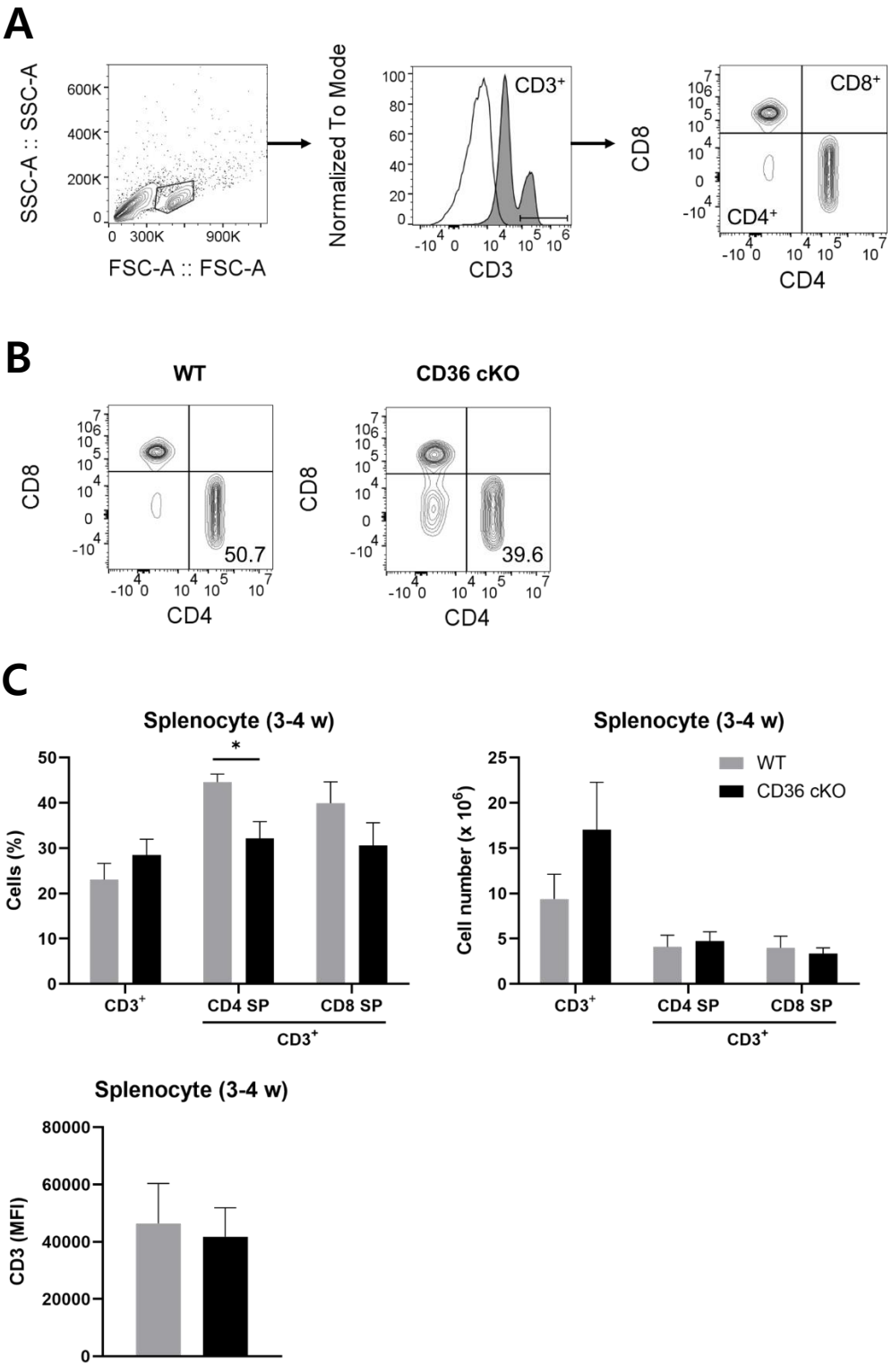
A
SSC-A :: SSC-A
FSC-A :: FSC-A
Normalized To Mode
CD3+
CD3
CD8
CD8+
CD4+
CD4
B
WT
CD36 cKO
CD8
CD4
50.7
39.6
C
Splenocyte (3-4 w)
Cells (%)
CD3+
CD4 SP
CD8 SP
Splenocyte (3-4 w)
Cell number (x 10^6)
WT
CD36 cKO
Splenocyte (3-4 w)
CD3 (MFI)

Figure 3. The phenotypes of splenic T cells in 3-4 week-old mice.

Flow cytometic analysis of splenocytes from 3-4 week-old CD36 cKO and WT mice. (A) Representative gating strategy is displayed. (B) Representative flow cytometric plots are shown. (C) The percentages, MFI, and cell numbers of splenocyte subsets are shown (n = 6-11 per group). Data are shown as mean ± SEM. * $p < 0.05$.

The reduced $CD3^+$ T cell population was only defect in the bone marrow from CD36 cKO 3-4 week-old mice.

To determine any defect of hematopoietic stem cells (HSCs) before thymic entry, I observed the phenotypes of bone marrow cells from CD36 cKO and WT mice by flow cytometry. The gating strategies of bone marrow cells are shown in Fig. 4A. $Lin^-Sca\text{-}1^+c\text{-}kit^+$ HSCs consist of long-term HSCs (LT-HSCs) and short-term HSCs (ST-HSCs) and they are distinguished by the expression of CD34. $CD34^-c\text{-}kit^+$ LT-HSCs, which have a long-term reconstitution capacity, differentiate into $CD34^+c\text{-}kit^+$ ST-HSCs that have a short-term reconstitution capacity. The expressions of CD34 and CD117 (c-kit) are maintained in MPPs which are derived from ST-HSCs [32]. MPPs generate $CD34^+c\text{-}kit^+$ CMPs and $CD34^+c\text{-}kit^{low}$ CLPs [33]. As progenitors mature, the expression of CD34 is lost. $CD34^-c\text{-}kit^-$ cells represent mature progenitors [34]. Flow cytometric results showed similar phenotypes between CD36 cKO and WT bone marrow cells except for $CD3^+$ frequency and MFI. The levels of $CD3^+$ frequency and MFI of CD36 cKO were reduced significantly by 0.7-fold and 0.57-fold, respectively (Fig. 4B, and C). The

expression of CD3 appears after DP stage of the thymus, and bone marrow cells entering the thymus do not express CD3 [35]. Taken together with the intact $CD3^+$ T cell population in the spleen, the results suggest that CD36 may be involved in homing to the bone marrow.

Figure 4.

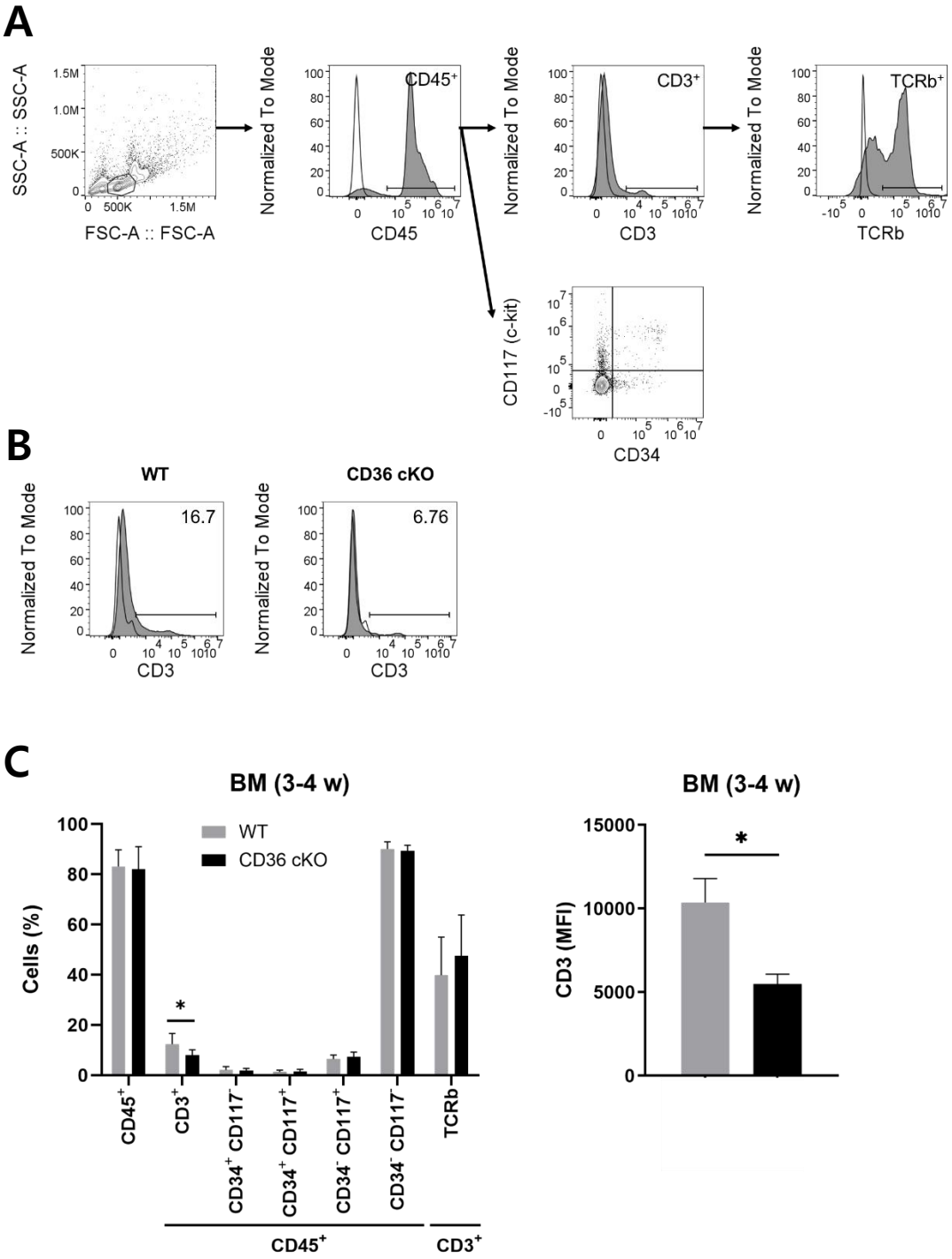
A
SSC-A :: SSC-A
FSC-A :: FSC-A
Normalized To Mode
CD45+
CD45
CD3+
CD3
TCRb+
TCRb
CD117 (c-kit)
CD34
B
WT
CD36 cKO
16.7
6.76
CD3
C
BM (3-4 w)
WT
CD36 cKO
Cells (%)
CD45+
CD3+
CD34+ CD117-
CD34+ CD117+
CD34- CD117+
CD34- CD117-
TCRb
CD3 (MFI)

Figure 4. The phenotypes of hematopoietic stem cells and T cell precursors in the bone marrow.

Flow cytometric analysis of bone marrow cells from 3-4 week-old CD36 cKO and WT mice. (A) Representative gating strategy is displayed. (B) Representative flow cytometry plots are shown. (C) The percentages and MFI of bone marrow cell subsets are shown (n = 7-8 per group). Data are shown as mean ± SEM. * $p < 0.05$.

The proliferation of activated CD36 cKO thymic T cells *in vitro* was increased in 3-4 week-old mice.

I investigated the proliferation of activated CD36 cKO thymic T cells. To assess the proliferation, thymocytes were labeled with CFSE. After CFSE staining, the cells were stimulated with IL-2, IL-2 and anti-CD3 mAb, or IL-2 and anti-CD3/28 mAb. The CFSE dilution was measured by flow cytometry on day 0, 3, and 5. The histogram plots were arbitrarily divided into 4 phases (Fig. 5A). Fig. 5B summarizes the flow cytometric data of Fig. 5A. CD36 cKO thymocytes stimulated with IL-2 and anti-CD3 mAb were significantly decreased by 0.1-fold and 0.37-fold in the phase 1 and 2 that were not or less divided and increased by 4.45-fold in the phase 4 compared with WT. CD36 cKO thymocytes with IL-2 and anti-CD3/28 mAb treatment were significantly downregulated by 0.07-fold and 0.19-fold in the phase 1 and 2 and upregulated by 3.5-fold in the phase 3, indicating that thymic T cells from CD36 cKO were more proliferative than those of WT (Fig. 5B). This results were confirmed using the CCK8 assay. The absorbance was measured on day 7. The cell

proliferation was significantly increased and nearly doubled in CD36 cKO thymic T cells (Fig. 5C).

To understand the underlying mechanisms of cell expansion, intracellular signaling molecules were assessed in thymic T cells. The flow cytometric gating strategy was shown in Fig. 6A. AKT and mTOR were more activated in 5 min, and ERK was more activated in 30 min upon anti-CD3 and anti-CD28 mAb stimulation, although the differences were not statistically significant. The percentage and MFI of CD36 cKO T cells were comparable to WT (Fig. 6B). The results suggest that CD36 cKO T cells got more activated upon CD3 complex stimulation.

Figure 5.

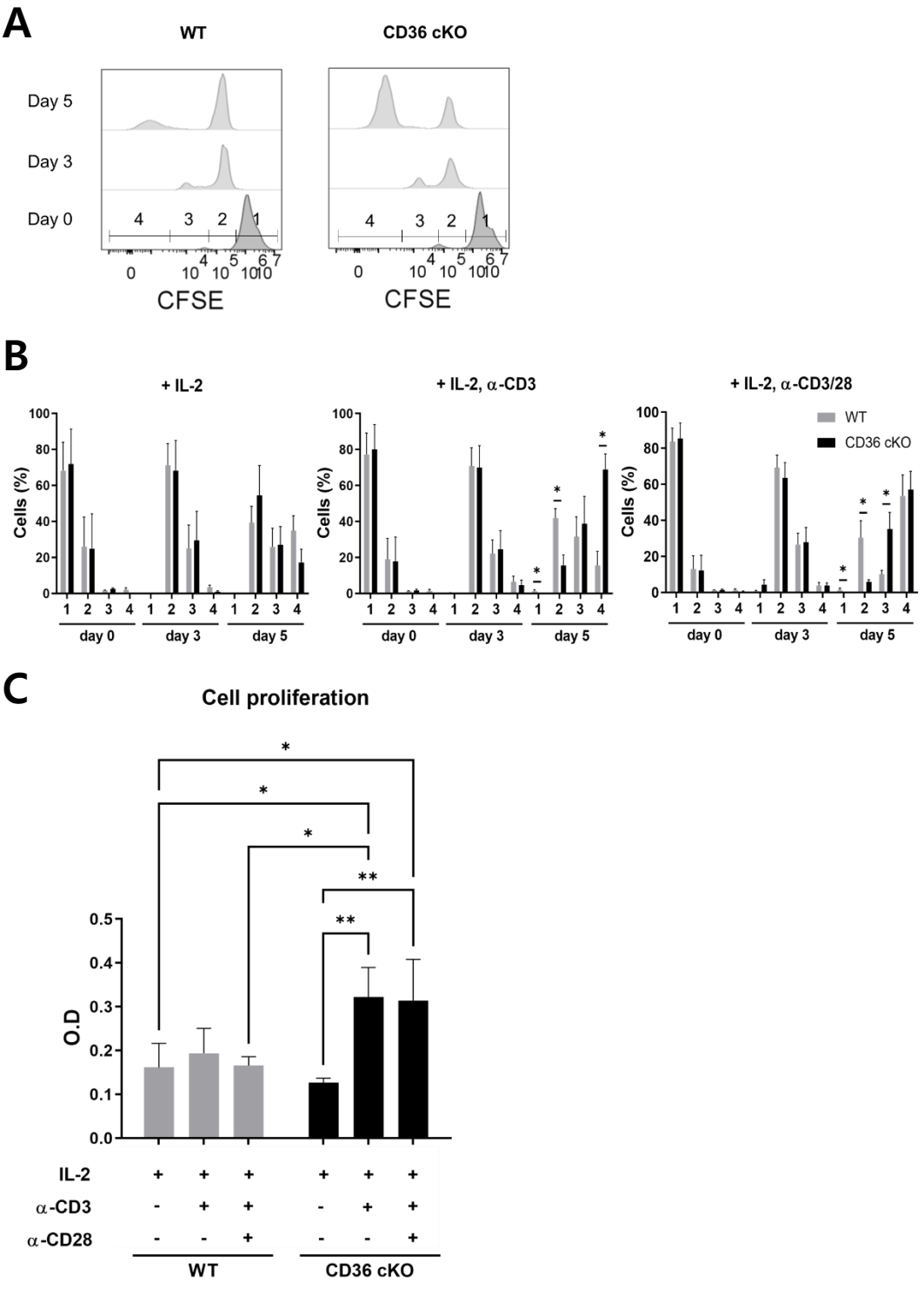
A
WT
CD36 cKO
Day 5
Day 3
Day 0
CFSE
CFSE
B
+ IL-2
+ IL-2, α-CD3
+ IL-2, α-CD3/28
WT
CD36 cKO
Cells (%)
day 0
day 3
day 5
C
Cell proliferation
O.D
IL-2
α-CD3
α-CD28
WT
CD36 cKO

Figure 5. Increased thymic T cell proliferation in CD36 cKO mice.

The proliferation of thymic T cells was assessed by CFSE labeling and CCK8 assay. After CFSE labeling, thymic T cells were stimulated in the presence of IL-2, anti-CD3, and anti-CD3/28 mAb and analyzed by flow cytometry on day 0, 3, and 5. (A) Representative flow cytometric plots are displayed. (B) The graphs show flow cytometric data of A (n = 4 – 10 per group). (C) Thymic T cells were cultured with IL-2, anti-CD3, and anti-CD3/28 mAb for 7 days and CCK8 assay was performed (n = 3 per group). CFSE, Carboxyfluorescein succinimidyl ester. CCK8, cell counting kit 8. Data are shown as mean ± SEM. * $p < 0.05$. ** $p < 0.01$.

Figure 6.

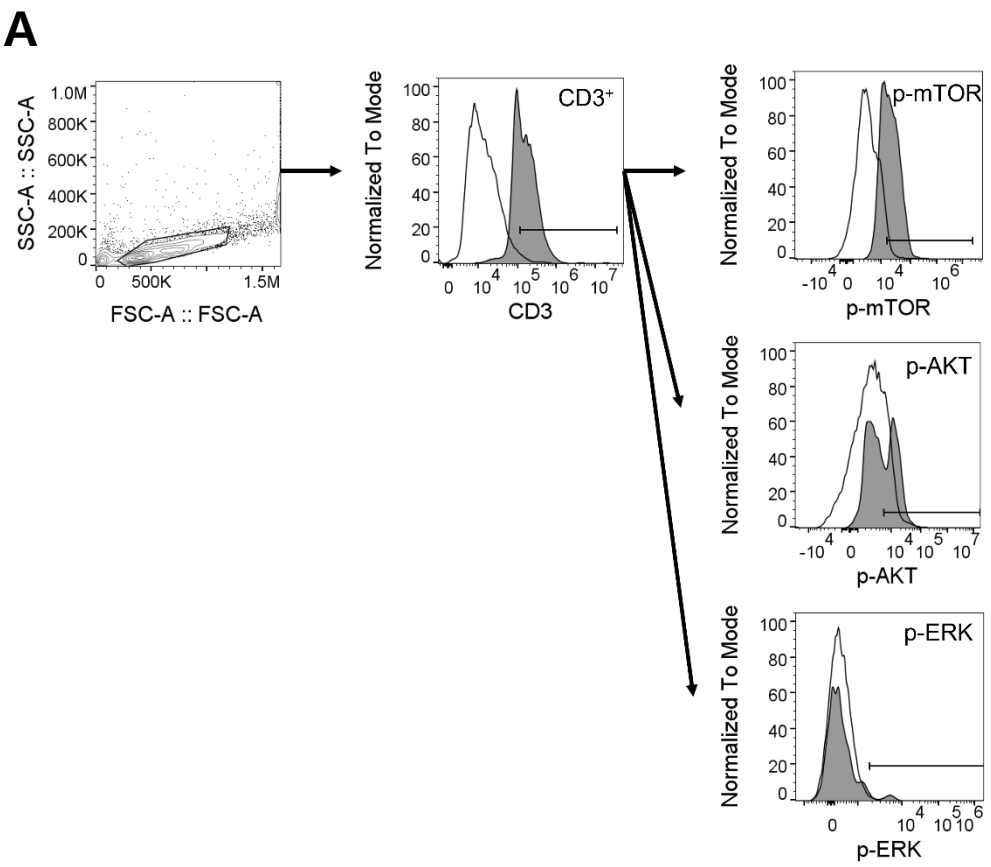
A
SSC-A :: SSC-A
1.0M
800K
600K
400K
200K
0
0
500K
1.5M
FSC-A :: FSC-A
Normalized To Mode
CD3+
CD3
p-mTOR
p-AKT
p-ERK

B

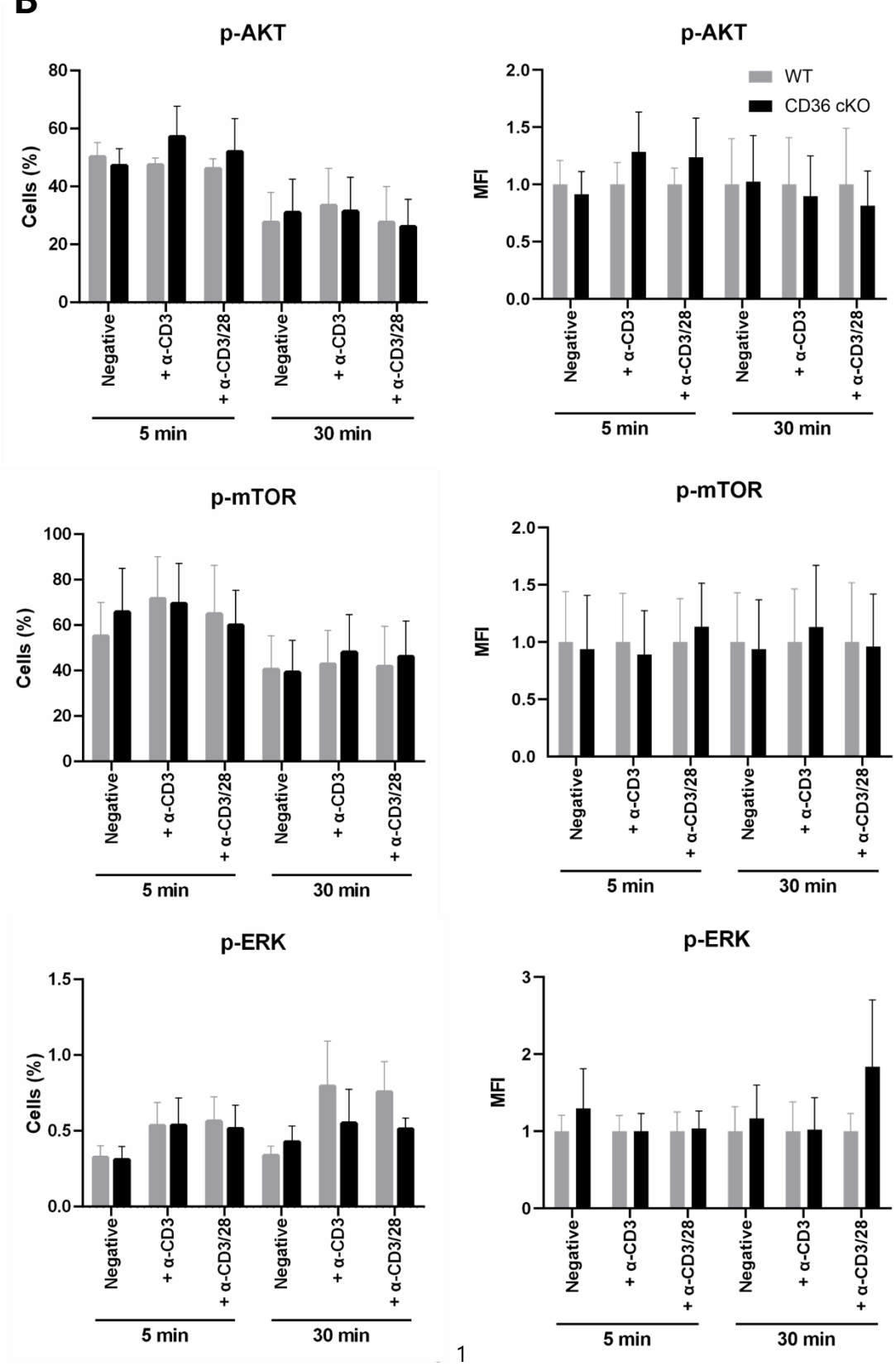
p-AKT
Cells (%)
80
60
40
20
0
Negative
+ α-CD3
+ α-CD3/28
Negative
+ α-CD3
+ α-CD3/28
5 min
30 min
p-AKT
MFI
2.0
1.5
1.0
0.5
0.0
WT
CD36 cKO
Negative
+ α-CD3
+ α-CD3/28
Negative
+ α-CD3
+ α-CD3/28
5 min
30 min
p-mTOR
Cells (%)
100
80
60
40
20
0
Negative
+ α-CD3
+ α-CD3/28
Negative
+ α-CD3
+ α-CD3/28
5 min
30 min
p-mTOR
MFI
2.0
1.5
1.0
0.5
0.0
Negative
+ α-CD3
+ α-CD3/28
Negative
+ α-CD3
+ α-CD3/28
5 min
30 min
p-ERK
Cells (%)
1.5
1.0
0.5
0.0
Negative
+ α-CD3
+ α-CD3/28
Negative
+ α-CD3
+ α-CD3/28
5 min
30 min
p-ERK
MFI
3
2
1
0
Negative
+ α-CD3
+ α-CD3/28
Negative
+ α-CD3
+ α-CD3/28
5 min
30 min

Figure 6. Expressions of phosphorylated (p)-AKT, p-mTOR, and p-ERK in thymic T cells.

For intracellular staining of p-AKT, mTOR, and ERK, thymic T cells were stimulated with α-CD3 and α-CD3/28 mAb for 5 and 30 min and immediately fixed. Expressions of p-AKT, p-mTOR, and p-ERK were determined by flow cytometry. (A) Representative gating strategy of p-AKT, p-mTOR, and p-ERK is displayed. (B) The percentages and MFI of p-AKT, p-mTOR, and p-ERK are shown (n = 3-5 per group). Data are shown as mean ± SEM.

The expression of selected chemokines and related molecules of CD36 cKO and WT mice in the thymus and bone marrow.

To understand underlying mechanisms in thymic T cell defect in CD36 cKO mice, mRNA sequencing was performed. Total RNA was extracted from CD36 cKO and WT thymocytes and bone marrow cells, and mRNA sequencing was performed. Venn diagram displayed significantly up-regulated, and down-regulated genes in the thymus and the bone marrow of CD36 cKO mice, compared with WT (Fig. 7A). One hundred and eight genes were up-regulated, and 49 genes were down-regulated in the thymus of CD36 cKO. CD36 cKO bone marrow cells highly expressed 183 genes and low expressed 103 genes. There were up-regulated 18 genes, down-regulated 8 genes, and contra-regulated 8 genes in the thymus, compared with bone marrow. Heat map indicated the expressions of the genes that are associated with immune response. It shows differential expression of chemokines and chemokine receptors such as *Ccl22,* and *Ccr7* (Fig. 7B). Interaction of the chemokines and chemokine receptors are essential for thymic development and selection [12]. The expression of selected chemokines and

chemokine receptors that mediate thymic development were shown in the table. The expression of *Ccl17* was significantly upregulated by 2.038-fold and the expression of *Ccl22* and *Ccr9* was significantly downregulated by 0.444- and 0.611-fold in CD36 cKO thymus, compared with WT thymus. The bone marrow of CD36 cKO had 1.862-fold higher expression of *Ccl17*, and 0.497- and 0.410-fold lower expression of *Ccr7* and *Ccr9* than that of WT (Fig. 7C). To confirm the results, I compared the selected chemokines' and chemokine receptors' gene expressions in the thymus and bone marrow by qRT-PCR. The expressions of *Ccl22* and *Ccr9* were significantly decreased by 0.28- and 0.58-fold in CD36 cKO thymocytes, compared with WT. *Ccl17* and *Ccl22* expressions were higher and *Ccr7* and *Ccr9* expressions were lower in CD36 cKO bone marrow than in WT, but the differences were not statistically significant (Fig. 7D). In addition, Bcl6, a transcription repressor, was significantly downregulated in the thymus from CD36 cKO. The results suggest that the deficiency of CD36 in T cells could change the expression of chemokines and their receptors, consequently affecting thymic T cell development and migration.

Figure 7.

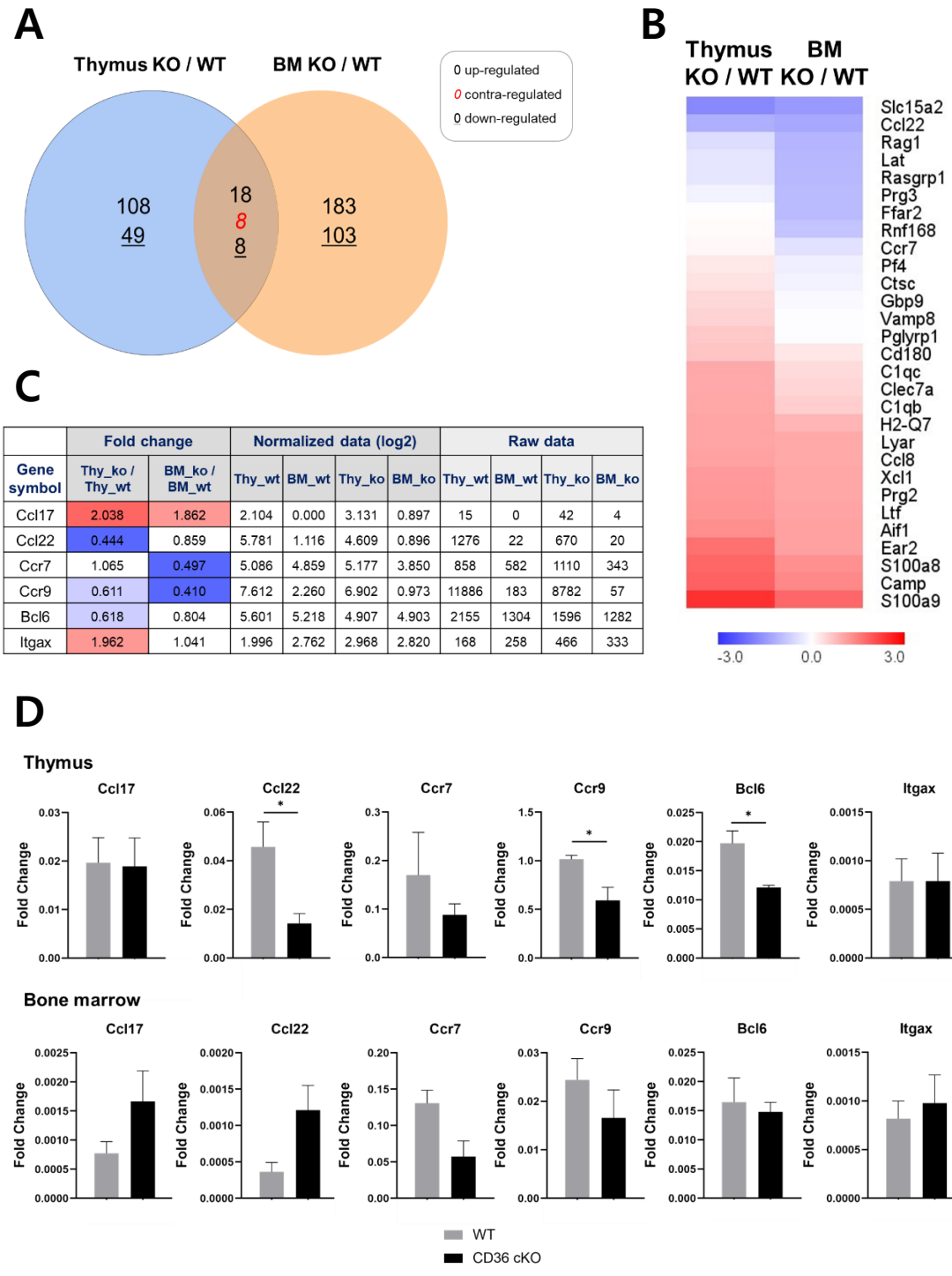

	Fold change		Normalized data (log2)				Raw data			
Gene symbol	Thy_ko / Thy_wt	BM_ko / BM_wt	Thy_wt	BM_wt	Thy_ko	BM_ko	Thy_wt	BM_wt	Thy_ko	BM_ko
Ccl17	2.038	1.862	2.104	0.000	3.131	0.897	15	0	42	4
Ccl22	0.444	0.859	5.781	1.116	4.609	0.896	1276	22	670	20
Ccr7	1.065	0.497	5.086	4.859	5.177	3.850	858	582	1110	343
Ccr9	0.611	0.410	7.612	2.260	6.902	0.973	11886	183	8782	57
Bcl6	0.618	0.804	5.601	5.218	4.907	4.903	2155	1304	1596	1282
Itgax	1.962	1.041	1.996	2.762	2.968	2.820	168	258	466	333

Figure 7. The gene expression of CD36 cKO thymus and bone marrow.

mRNA sequencing of thymocytes and bone marrow cells from CD36 cKO and WT mice was performed. Analysis data from RNA-seq results are shown (n = 1 per group). (A) Venn diagram indicates significantly up, contra, and down-regulated genes between the thymus and bone marrow. (B) Heat map for immune response genes. (C) Differential expressions of chemokine and chemokine receptor genes (*Ccl17, Ccl22, Ccr7, Ccr9, Bcl6, and Itgax*) between CD36 cKO and WT. (D) Expression of *Ccl17, Ccl22, Ccr7*, *Ccr9, Bcl6, and Itgax* from the thymus and bone marrow was analyzed by qRT-PCR (n = 4-8 per group). Data are shown as mean ± SEM. * $p < 0.05$. qRT-PCR, quantitative real-time PCR.

Discussion

This study demonstrates that DN, DN3, $CD3^+$ DP and CD8 SP T cells significantly increased and DN4, total DP, $CD3^-$ DP and CD4 SP T cells significantly decreased in the thymus of 3-4 week-old T cell-specific CD36 cKO mice, and that activated thymic $CD3^+$ T cells from CD36 cKO were more proliferative, compared with those of WT.

Thymic T cells develop as they migrate within the cortex and the medulla of the thymus and interact with stromal cells. Chemokines and their receptors are involved in thymocyte migration and differentiation. Chemokines known as essential chemoattractant molecules for migration are expressed in the thymus at various developmental stages [36]. The chemokine receptor CCR9 begins to be expressed at DN3 thymocytes. Its ligand, CCL25, is expressed in the thymic cortex where DN thymocytes are located [37]. The expression of CCR9 is increased during the transition from DN to DP [38]. CCR9 expression is induced by pre-TCR signals that lead to expansion and differentiation to the DP thymocytes. CCR9 is subsequently upregulated between the DN4 and DP stages, and functions in the localization of thymocytes during

maturation [39]. Thymocytes, which downregulate CCR9 expression, impair migration toward the subcapsular zone where they undergo their TCR β-, γ-, and δ-chain gene recombination [40]. In this study, mRNA sequencing data showed that the expression of CCR9 was down-regulated by 0.611-fold in the thymus of 3-4 week-old CD36 cKO mice than WT. The expression of CCR9 was significantly decreased by 0.58-fold in CD36 cKO thymocytes by qRT-PCR, compared with WT. These results suggest that a decrease of DN4 thymocytes from CD36 cKO mice might be associated with the downregulation of CCR9.

Transcription repressor Bcl6 induces pre-TCR signaling and is required for differentiation to DP. Bcl6 deficiency in thymocytes dysregulate β-selection and increase cell death of the DN4 in fetus and adult [41]. RNA sequencing results showed 0.618-fold downregulation of *Bcl6* in the thymus. The expression of *Bcl6* in qRT-PCR was significantly downregulated by 0.615-fold in CD36 cKO thymus, compared with WT thymus (Fig.7D). None of the genes tested in the study was significantly changed in its expression in the bone marrow. Further experiments are needed to evaluate cell death at developmental stages. Since my RNA

sequencing has limitations that have been performed by the entire thymus tissue, further research is also required to analyze gene expressions in the T cell subsets at each developmental stage.

Thymic T cells from CD36 cKO mice were more proliferative than WT, but the percentages and MFI of p-AKT$^+$, p-mTOR$^+$, and p-ERK$^+$ CD36 cKO T cells were comparable to WT. A recent study reported that integrin αX (CD11c) is contributed to late-stage T cell development and maintains T cell survival. CD11c deficiency showed increasing apoptosis of CD3$^+$ thymocytes, but not DN cells [42]. *Itgax* expression in RNA-seq data was upregulated by 1.962-fold. As integrins play important roles in TCR signaling thymic differentiation [43], the increase of CD11c might enforce the immune synapses between T cells and APCs, consequently enhance the T cell proliferation. However, the qRT-PCR results were not statistically significant. The thymus of CD36 cKO displayed 0.987-fold decrease in *Itgax* expression compared with WT (Fig.7D). Given the specific contribution of CD11c to distinct developmental stages, additional study is needed to analyze each developmental stage using flow cytometry.

Recent human studies indicate that CD36 plays a crucial role in the pathogenesis of tumors and autoimmune diseases. The function of CD36 that mediated fatty acid uptake has been correlated with progression and metastasis of various human tumors, including breast cancer [44] and hepatocellular carcinoma [45]. The loss of CD36 has been associated with the development of colorectal cancer, where CD36 acts as a tumor suppressor and inhibits aerobic glycolysis [46]. In autoimmune diseases, CD36 as a scavenger receptor contributes to the immunopathogenesis of Kawasaki disease, an autoimmune-like vasculitis affecting the coronary arteries in childhood. CD36 plays a role in clearing cellular debris and then activating the inflammasome pathway [47]. CD36 is implicated in clearing myelin debris and suppressing neuroinflammation in demyelinating disorders such as multiple sclerosis [48]. Thus, the physiological roles of CD36 in T cells should be further investigated in tumor and autoimmune disease models.

In conclusion, this study suggests that CD36 is a potential contributor to the transition from DN3 to SP cells in thymic T cell development and has a regulatory function in

proliferation. The results imply the potential role of CD36 in T cells in pediatric tumors and autoimmune diseases.

References

1. Glatz, J.F.C. and J. Luiken, *Dynamic role of the transmembrane glycoprotein CD36 (SR-B2) in cellular fatty acid uptake and utilization.* J Lipid Res, 2018. **59**(7): p. 1084-1093.

2. Febbraio, M., D.P. Hajjar, and R.L. Silverstein, *CD36: a class B scavenger receptor involved in angiogenesis, atherosclerosis, inflammation, and lipid metabolism.* J Clin Invest, 2001. **108**(6): p. 785-91.

3. Chen, Y., et al., *CD36, a signaling receptor and fatty acid transporter that regulates immune cell metabolism and fate.* J Exp Med, 2022. **219**(6).

4. Febbraio, M., et al., *A null mutation in murine CD36 reveals an important role in fatty acid and lipoprotein metabolism.* J Biol Chem, 1999. **274**(27): p. 19055-62.

5. Silverstein, R.L. and M. Febbraio, *CD36, a scavenger receptor involved in immunity, metabolism, angiogenesis, and behavior.* Sci Signal, 2009. **2**(72): p. re3.

6. Woo, M.S., et al., *Cell Surface CD36 Protein in Monocyte/Macrophage Contributes to Phagocytosis during the Resolution Phase of Ischemic Stroke in Mice.* J Biol Chem, 2016. **291**(45): p. 23654-23661.

7. Urban, B.C., N. Willcox, and D.J. Roberts, *A role for CD36 in the regulation of dendritic cell function.* Proc Natl Acad Sci U S A, 2001. **98**(15): p. 8750-5.

8. Ma, X., et al., *CD36-mediated ferroptosis dampens intratumoral CD8(+) T cell effector function and impairs their antitumor ability.* Cell Metab, 2021. **33**(5): p. 1001-1012.e5.

9. Wang, H., et al., *CD36-mediated metabolic adaptation supports regulatory T cell survival and function in tumors.* Nat Immunol, 2020. **21**(3): p. 298-308.

10. Shah, D.K. and J.C. Zúñiga-Pflücker, *An overview of the intrathymic intricacies of T cell development.* J Immunol, 2014. **192**(9): p. 4017-23.

11. Seita, J. and I.L. Weissman, *Hematopoietic stem cell: self-renewal versus differentiation.* Wiley Interdiscip Rev Syst Biol Med, 2010. **2**(6): p. 640-53.

12. Lancaster, J.N., Y. Li, and L.I.R. Ehrlich, *Chemokine-Mediated Choreography of Thymocyte Development and Selection.* Trends Immunol, 2018. **39**(2): p. 86-98.

13. Taghon, T., et al., *Developmental and molecular characterization of emerging beta- and gammadelta-selected pre-T cells in the adult mouse thymus.* Immunity, 2006. **24**(1): p. 53-64.

14. Dutta, A., B. Zhao, and P.E. Love, *New insights into TCR β-selection.* Trends Immunol, 2021. **42**(8): p. 735-750.

15. Ciofani, M. and J.C. Zúñiga-Pflücker, *The thymus as an inductive site for T lymphopoiesis.* Annu Rev Cell Dev Biol, 2007. **23**: p. 463-93.

16. Carpenter, A.C. and R. Bosselut, *Decision checkpoints in the thymus.* Nat Immunol, 2010. **11**(8): p. 666-73.

17. Starr, T.K., S.C. Jameson, and K.A. Hogquist, *Positive and negative selection of T cells.* Annu Rev Immunol, 2003. **21**: p. 139-76.

18. Love, P.E. and A. Bhandoola, *Signal integration and crosstalk during thymocyte migration and emigration.* Nat Rev Immunol, 2011. **11**(7): p. 469-77.

19. Lim, S.A., et al., *Lipid metabolism in T cell signaling and function.* Nat Chem Biol, 2022. **18**(5): p. 470-481.

20. Li, H., et al., *High-Fat Diet from Weaning until Early Adulthood Impairs T Cell Development in the Thymus.* Lipids, 2020. **55**(1): p. 35-44.

21. Gulvady, A.A., et al., *Glycerol-3-phosphate acyltransferase-1 gene ablation results in altered thymocyte lipid content and reduces thymic T cell production in mice.* Lipids, 2013. **48**(1): p. 3-12.

22. Qu, P., et al., *Critical roles of lysosomal acid lipase in T cell development and function.* Am J Pathol, 2009. **174**(3): p. 944-56.

23. Son, N.H., et al., *Endothelial cell CD36 optimizes tissue fatty acid uptake.* J Clin Invest, 2018. **128**(10): p. 4329-4342.

24. Shi-Bai, Z., et al., *TIPE2 expression is increased in peripheral blood mononuclear cells from patients with rheumatoid arthritis.* Oncotarget, 2017. **8**(50): p. 87472-87479.

25. Yuan, J., R.B. Crittenden, and T.P. Bender, *c-Myb promotes the survival of CD4+CD8+ double-positive thymocytes through upregulation of Bcl-xL.* J Immunol, 2010. **184**(6): p. 2793-804.

26. Noor, S., et al., *CCR7-dependent immunity during acute Toxoplasma gondii infection.* Infect Immun, 2010. **78**(5): p. 2257-63.

27. Huang, Y., et al., *Abrogation of CC chemokine receptor 9 ameliorates ventricular remodeling in mice after myocardial infarction.* Sci Rep, 2016. **6**: p. 32660.

28. Monick, M.M., et al., *Respiratory syncytial virus synergizes with Th2 cytokines to induce optimal levels of TARC/CCL17.* J Immunol, 2007. **179**(3): p. 1648-58.

29. Yashiro, T., et al., *A transcription factor PU.1 is critical for Ccl22 gene expression in dendritic cells and macrophages.* Sci Rep, 2019. **9**(1): p. 1161.

30. Trobridge, P.A., K.A. Forbush, and S.D. Levin, *Positive and negative selection of thymocytes depends on Lck interaction with the CD4 and CD8 coreceptors.* J Immunol, 2001. **166**(2): p. 809-18.

31. Weerkamp, F., K. Pike-Overzet, and F.J. Staal, *T-sing progenitors to commit.* Trends Immunol, 2006. **27**(3): p. 125-31.

32. Cheng, H., Z. Zheng, and T. Cheng, *New paradigms on hematopoietic stem cell differentiation.* Protein Cell, 2020. **11**(1): p. 34-44.

33. Almotiri, A., A. Abdelfattah, and N.P. Rodrigues, *Flow Cytometry Analysis of Hematopoietic Stem/Progenitor Cells and Mature Blood Cell Subsets in Atherosclerosis.* Methods Mol Biol, 2022. **2419**: p. 583-595.

34. Hughes, M.R., et al., *A sticky wicket: Defining molecular functions for CD34 in hematopoietic cells.* Exp Hematol, 2020. **86**: p. 1-14.

35. Ceredig, R. and T. Rolink, *A positive look at double-negative thymocytes.* Nat Rev Immunol, 2002. **2**(11): p. 888-97.

36. Savino, W., et al., *Molecular mechanisms governing thymocyte migration: combined role of chemokines and extracellular matrix.* J Leukoc Biol, 2004. **75**(6): p. 951-61.

37. Hu, Z., J.N. Lancaster, and L.I. Ehrlich, *The Contribution of Chemokines and Migration to the Induction of Central Tolerance in the Thymus.* Front Immunol, 2015. **6**: p. 398.

38. Wurbel, M.A., et al., *Mice lacking the CCR9 CC-chemokine receptor show a mild impairment of early T- and B-cell development and a reduction in T-cell receptor gammadelta(+) gut intraepithelial lymphocytes.* Blood, 2001. **98**(9): p. 2626-32.

39. Krishnamoorthy, V., et al., *Repression of Ccr9 transcription in mouse T lymphocyte progenitors by the Notch signaling pathway.* J Immunol, 2015. **194**(7): p. 3191-200.

40. Wurbel, M.A., B. Malissen, and J.J. Campbell, *Complex regulation of CCR9 at multiple discrete stages of T cell development.* Eur J Immunol, 2006. **36**(1): p. 73-81.

41. Solanki, A., et al., *The transcriptional repressor Bcl6 promotes pre-TCR-induced thymocyte differentiation and attenuates Notch1 activation.* Development, 2020. **147**(19).

42. Hou, L. and K. Yuki, *CD11c regulates late-stage T cell development in the thymus.* Front Immunol, 2022. **13**: p. 1040818.

43. Burbach, B.J., et al., *T-cell receptor signaling to integrins.* Immunol Rev, 2007. **218**: p. 65-81.

44. Pascual, G., et al., *Targeting metastasis-initiating cells through the fatty acid receptor CD36.* Nature, 2017. **541**(7635): p. 41-45.

45. Luo, X., et al., *The fatty acid receptor CD36 promotes HCC progression through activating Src/PI3K/AKT axis-dependent aerobic glycolysis.* Cell Death Dis, 2021. **12**(4): p. 328.

46. Fang, Y., et al., *CD36 inhibits β-catenin/c-myc-mediated glycolysis through ubiquitination of GPC4 to repress colorectal tumorigenesis.* Nat Commun, 2019. **10**(1): p. 3981.

47. Guo, M.M., et al., *CD36 is Associated With the Development of Coronary Artery Lesions in Patients With Kawasaki Disease.* Front Immunol, 2022. **13**: p. 790095.

48. Grajchen, E., et al., *CD36-mediated uptake of myelin debris by macrophages and microglia reduces neuroinflammation.* J Neuroinflammation, 2020. **17**(1): p. 224.

국문요약

배경: 지방산 수송체이자 scavenger 수용체로도 알려진 CD36 은 신호전달물질 및 지질전달체로 기능을 하는 막관통 분자이다. CD36 은 산화된 저밀도 지단백, 장쇄 지방산, DAMP, PAMP 등을 ligand 로 한다. CD36 은 지방세포, 근육세포, 내피세포 뿐만 아니라 혈소판, 적혈구, 대식세포, 수지상세포, T 세포와 같은 면역 세포에서도 발현한다. 면역 세포에서 발현하는 CD36 은 면역 대사에 역할을 하는 것으로 알려져 있으나 T 세포 발달에서의 기능 아직 충분히 밝혀지지 않았다.

방법: CD36-floxed 마우스와 Lck-cre 마우스를 교배하여 T 세포에서 CD36 이 결핍된 마우스를 제작하였다. 3-4 주령과 5-8 주령 T 세포 특이적 CD36 제거 마우스의 흉선, 비장, 골수 세포를 유세포분석을 통해 분석하였다. 흉선 T 세포를 인터루킨 2 와 항 CD3, 항 CD28 단일클론항체를 처리하여 CFSE 표지와 CCK8 으로 T 세포 증식을 평가하였다. T 세포 증식과 관련된 기작을 알아보고자 신호전달 물질인 AKT, mTOR 와 ERK 의 활성화를 유세포분석으로 관찰하였다. 흉선과 골수 세포에서 RNA 를 추출하여 mRNA 시퀀싱과 qRT-PCR 을 진행하였다.

결과: 3-4 주령 CD36 cKO 는 흉선 내 $CD3^+$, DN, DN3, $CD3^+$ DP 및 CD8 SP 세포의 증가와 $CD3^-$, DP, DN4, $CD3^-$ DP 및 CD4 SP 세포의 감소를 보였다. CD36 cKO 비장세포에서 CD4 SP 세포의 빈도는 WT 보다 낮았다. CD36 cKO 마우스에서 $CD3^+$ 골수 세포의 빈도와 MFI 는 WT 보다 낮았다. CD36 cKO 의 흉선 T 세포는 WT 보다 더 증식했다. mRNA 시퀀싱 데이터에서 *Ccl17* 과 *Ccr7* 의 발현이 상향 조절되고, *Ccl22* 와 *Ccr9* 의 발현은 CD36 cKO 흉선에서 하향 조절되었다. qRT-PCR 을 통해 WT 에 비해 CD36 cKO 흉선 세포에서 *Ccl22* 와 *Ccr9* 의 발현이 유의하게 감소하는 것을 확인하였다. CD36 cKO 골수에서 WT 보다 *Ccl17* 과 *Ccl22* 발현이 높았고 *Ccr7* 과 *Ccr9* 발현은 낮았지만 통계적으로 유의하지 않았다.

결론: 3-4 주령의 CD36 cKO 는 DN3 에서 DN4 로의 분화에 결함이 있다. CD36 cKO 흉선 T 세포는 WT 보다 더 빠르게 증식했다. 흉선 T 세포의 발달 문제는 케모카인과 케모카인 수용체의 발현 변화에서 비롯되었을 수 있다. 이 연구는 CD36 이 DN 단계부터 흉선 T 세포 발달에 잠재적인 역할을 하며 흉선 T 세포 증식에 조절 기능을 가지고 있음을 시사한다.